

A Biological Nanomachine at Work: Watching the Cellulosome Degrade Crystalline Cellulose

Manuel Eibinger,[¶] Thomas Ganner,[¶] Harald Plank,* and Bernd Nidetzky*Cite This: *ACS Cent. Sci.* 2020, 6, 739–746

Read Online

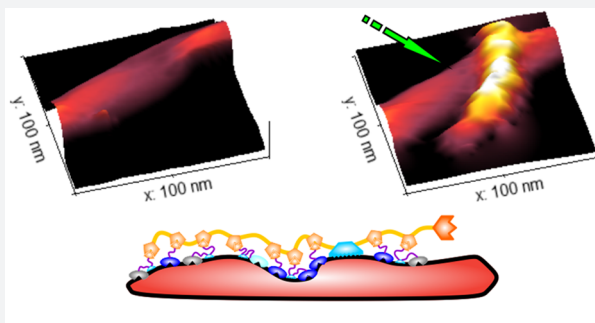
ACCESS |

Metrics & More

Article Recommendations

Supporting Information

ABSTRACT: The cellulosome is a supramolecular multienzymatic protein complex that functions as a biological nanomachine of cellulosic biomass degradation. How the megadalton-size cellulosome adapts to a solid substrate is central to its mechanism of action and is also key for its efficient use in bioconversion applications. We report time-lapse visualization of crystalline cellulose degradation by individual cellulosomes from *Clostridium thermocellum* by atomic force microscopy. Upon binding to cellulose, the cellulosomes switch to elongated, even filamentous shapes and morph these dynamically at below 1 min time scale according to requirements of the substrate surface under attack. Compared with noncomplexed cellulases that peel off material while sliding along crystalline cellulose surfaces, the cellulosomes remain bound locally for minutes and remove the material lying underneath. The consequent roughening up of the surface leads to an efficient deconstruction of cellulose nanocrystals both from the ends and through fissions within. Distinct modes of cellulose nanocrystal deconstruction by nature's major cellulase systems are thus revealed.



The cellulosome attacks a cellulose crystal

INTRODUCTION

The spatial organization of enzymes on nanoscale scaffolds is a fundamental principle of nature,^{1,2} and of bioengineering strategies inspired by it,^{3–6} to enhance the efficiency of catalytic reaction networks via proximity effects. A unique scaffold-assisted supramolecular assembly of enzymes is presented by the plant cell wall degrading apparatus of select anaerobic bacteria termed “the cellulosome”. The cellulosome is a megadalton-size protein complex built from multiple enzymatic subunits anchored on a noncatalytic scaffold protein, as illustrated in Figure 1.^{7–9}

Cellulosomal enzyme systems comprise a consortium of activities, mainly glycoside hydrolases, required for the complete depolymerization of the major polysaccharides in plant biomass, cellulose, and hemicellulose.^{9,10} The different enzymes exhibit biochemical synergy in attacking the complex composite structures present in lignocellulosic substrates undergoing degradation.¹¹ Enzyme synergy likely benefits from proximity effects.^{7–9,12} However, in order to respond to changing requirements on enzyme synergy due to spatiotemporal variations in substrate morphology and chemical composition, the cellulosome must be able to flexibly adjust its supramolecular structure to allow for a dynamic use of proximity. Conformational plasticity, revealed in experiment^{9–15} and by modeling,^{15,16} therefore, is fundamental to the cellulosome's mode of action. The cellulosome represents the paradigm for the deconstruction of a recalcitrant solid biomaterial by an enzymatic nanomachine. Besides its broad

biological importance, the cellulosome also has considerable industrial significance. It shows particular efficiency in the degradation of cellulosic substrates^{10,17,18} and so could play a central role in the development of advanced biorefinery and nanobiotechnology applications.^{5,19,20}

Use of a molecular dissection-and-reconstruction approach allowed for a structural characterization of the various isolated modules associated with the cellulosome and enabled an investigation of the assembly and the function of multimodular cellulosomal fragments (reviewed in refs 7–9). The intercohesin linker regions in these fragments were shown to have high structural flexibility^{13,21,22} and nanomechanical stability.²³ A “molecular spring” function of the linkers was proposed,¹³ entailing an ability to dynamically adjust the linker length according to topological requirements of the substrate.²⁴ Despite these insights into higher-order architecture and conformational adaptability of the cellulosome, evidence on the dynamic properties of the complete nanomachine particularly with regard to solid substrate deconstruction is not available. Early work by electron microscopy revealed basic

Received: January 15, 2020

Published: May 6, 2020



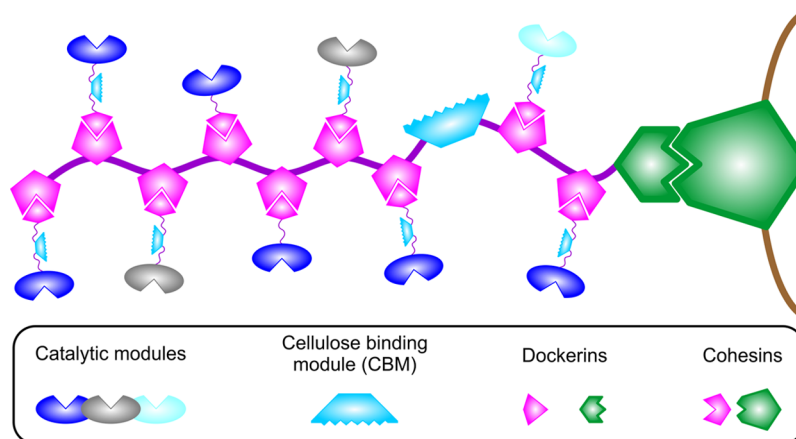


Figure 1. The cellulosome nanomachine for cellulose degradation. Supramolecular assembly of the cellulosome complex involves interaction from dockerin modules in the different catalytic entities with cohesin modules in a noncatalytic scaffolding protein. A prototypical scaffoldin from the cellulose-degrading bacterium *Clostridium thermocellum* has 9 cohesin modules. Carbohydrate binding modules promote binding to substrate. The cellulosome is tethered noncovalently to the bacterial cell surface (indicated in brown) via additional dockerin-cohesin interactions.

characteristics of the cellulosome's ultrastructure^{25,26} but essentially lacked in ability to capture protein conformational dynamics under native-like conditions of action and in real time.

Here, we analyze the interaction of individual *C. thermocellum* cellulosomes with crystalline cellulose in detail, applying fast time-lapse AFM with lateral and temporal resolutions suitable for tracking single protein complexes on the cellulose surface. Besides visualizing the ultrastructural dynamics of the cellulosomes in a liquid environment at the minute time scale, we were also able to study effects on substrate deconstruction. We observe fundamental differences in the way nanocrystalline cellulose is degraded by the cellulosomes as compared with degradation of the same substrate by cellulases that do not assemble into protein complexes and act as an ensemble of free enzymes. The paradigmatic "slide-and-peel" mode of removing layers of surface material by the noncomplexed cellulases^{17,27–29} is contrasted with an alternative "sit-and-dig" mode of crystalline surface degradation by the cellulosomes. Our results provide mechanistic interpretation for the previously observed cooperativity between the cellulosome and cellulases^{17,18} in releasing soluble sugars from cellulosic substrates.

RESULTS AND DISCUSSION

Single-Molecule Characterization of Surface-Bound Cellulosomes with Atomic Force Microscopy. We used cellulosomes purified from the culture supernatant of *C. thermocellum* grown on microcrystalline cellulose.^{17,30} We chose the *C. thermocellum* cellulosome because it represents the prototype for this class of biological nanomachines.^{7–9} The cellulosomes produced under these conditions, on average, are fully formed regarding their subunit composition and incorporate a complete set of cellulose-degrading enzyme activities.^{10,31} Thus, they are well suited for the proposed AFM study of crystalline cellulose degradation. The *C. thermocellum* cellulosome is usually anchored in the bacterial cell wall. However, a significant portion of it is released to supernatant from which it can be recovered conveniently.^{17,32} We therefore did not consider other cellulosome systems, less well characterized than the one from *C. thermocellum*, that may originally lack the attachment to the cell wall.^{7,8} We initially

analyzed the cellulosomes in the absence of cellulose substrate. For that, we took advantage of their adsorption onto the wafer used as support for the AFM measurements. We recorded AFM data of the adsorbed cellulosomes (~50 single molecules, ~480 subunits) in the dried state. We show in Figure S1 that individual cellulosomes could be made out definitely on the wafer surface. The ultrastructure of these cellulosomes was well resolved into a set of roughly spherical particles of similar size (10–20 nm in diameter; Figure S1A,B). We applied a height cutoff of ~1 nm to the identification of the spherical particles. Each particle likely represents an individual subunit of the cellulosome.^{7–9,33} We calculated that the surface area covered by an individual cellulosome approximates around 1500 nm². A similar area/cellulosome can be calculated from electron microscopy images of an earlier publication.³⁴ We show that the number of subunits/single cellulosome was centered at around 9 (Figure S1C), as anticipated for the fully formed protein complex (Figure 1). The experimental distribution of subunits/single cellulosome (Figure S1D) is attributed to (i) a natural or preparation-dependent variation in the loading of catalytic subunits on the scaffold protein or (ii) a variable amount of noncatalytic modules present in the individual cellulosomes as-isolated.³⁵ Single cellulosomes adsorbed on the wafer surface adopted various, apparently irregular shapes (Figure S1A,B). Internal compactness due to extensive intersubunit packing was however a prominent feature shared by the majority of them.

Based on the evidence from the dried-state characterization of the cellulosomes, we moved to AFM analysis in liquid environment. Interactions between the sample and the AFM probe are dominated by different forces in liquid as compared with the dried state.³⁶ A special measurement setup was therefore required. Using a temperature-controlled AFM liquid cell equipped with a laboratory-built liquid injection unit,²⁹ we were able, after extensive method development and optimization, to obtain high-quality image sequences of individual cellulosomes at 50 °C. Our choice of reaction conditions reflects compromise between optimum activity of the cellulosomes (~60–65 °C,^{11,17}) and practical challenge of AFM measurements at thus elevated temperature. Other researchers have used 55 °C¹⁷ or even lower temperatures³² to study the *C. thermocellum* cellulosome. We discovered after

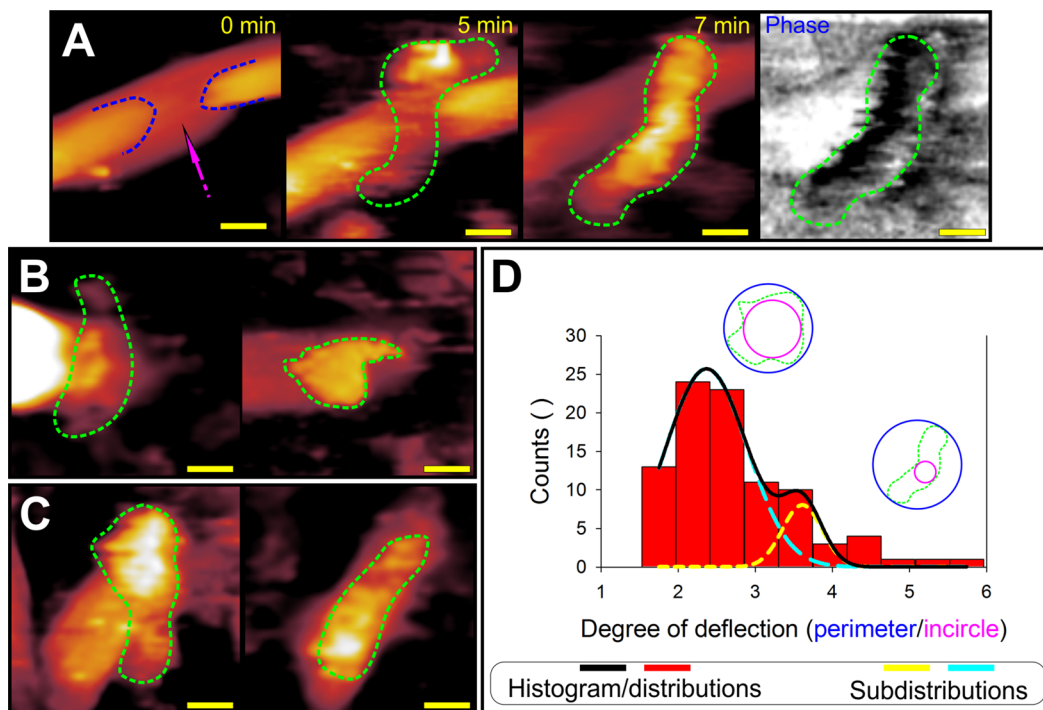


Figure 2. Single-molecule visualization of the cellulosome interacting with crystalline cellulose under native-like reaction conditions. (A) Time-lapse AFM observation at 50 °C of a single cellulosome (outlined in green) adsorbing to a cellulose nanocrystal. Image acquisition rate was 0.5 min⁻¹, and identification of cellulosomes was supported by material-property-sensitive phase information. (B,C) Cellulosomes adsorbed to the ends of cellulose nanocrystals (B) adopt bent (sickle-like) and compact shapes while those adsorbed on the top surface of crystals (C) adopt elongated (filamentous) shapes. (D) Individual cellulosomes ($N = 60$) were tracked and the ratios of the inscribed and circumscribed circles were calculated to give the “degree of deflection” (DoD). Values of DoD approaching unity indicate a circular shape while larger DoD values indicate a more elongated appearance. All AFM experiments were conducted at 50 °C with a resolution of ≤ 2 nm/pix. Scale bars are 50 nm.

preliminary experiments that hydrophobic modification of the AFM probe with octadecyltrichlorosilane significantly improved image quality at elevated temperature (see *Supporting Information* “Modification of AFM tips” for details), thus enabling single-molecule study of the cellulosome during its attack on cellulosic substrate for the first time (Figure 2). However, despite all measures and precautions taken, about 20% of the frames recorded showed cellulosomes that were apparently distorted and did not have exactly defined borders. Problems with stable imaging of the cellulosome likely have their origin in the high conformational flexibility of the cellulosome itself,¹⁴ a difficult complication encountered in the AFM analysis of other biomolecules,^{37,38} as well as in the challenging AFM measurements at elevated temperature.³⁸ However, it is important to emphasize that for a cellulosome to appear distorted must not be equated with it being damaged or destroyed. Careful control experiments revealed clear distinction between damaged or mechanically unfolded cellulosomes and temporary imaging artifacts (Figure S2). On the basis of these results, a range of parameters of the AFM experiment could be established that largely exclude damage to the cellulosomes in consequence of measurement (see *Supporting Information* “Identification of cellulosomes during time-lapse AFM experiments” for details). Using height information combined with phase information from the AFM measurements, single cellulosomes were unambiguously identified on the cellulose surface (Figure 2A; see *Supporting Information* “Identification of cellulosomes during time-lapse AFM experiments”). To monitor the enzymatic process by AFM, we used cellulose nanocrystals adsorbed on the wafer

surface as the substrate. The cellulose nanocrystals used represent the highly crystalline material of the natural cellulose allomorph I β .²⁹ The small size of these cellulose nanocrystals and relatively simple morphology render the cellulose nanocrystals particularly suitable for the study of crystalline cellulose degradation by the cellulosome. Intrinsic characteristics of the deconstruction process, unmasked from the convoluted effect of protein size on substrate accessibility in larger microcrystalline cellulose particles^{17,39,40} or lignocellulosic fibers,³² are thus revealed. We considered that as a side product of their preparation, the nanocrystals exhibit sulfate half-ester groups on their surface. The sulfate groups can affect the enzyme interaction with cellulose and may lead to a slowed rate of the hydrolysis when present in large abundance.⁴¹ We were careful, therefore, to obtain cellulose nanocrystals with only a small sulfate substitution degree on the surface (see *Supporting Information* “Characterization of cellulose nanocrystals”). Additionally, as shown later in more detail, we confirmed activity of the cellulosome toward releasing soluble sugars from the cellulose nanocrystals used.

AFM Study of the Cellulosome on the Cellulose Surface. Analyzing 60 cellulosomes individually (a selection thereof is shown in Figure 2A–D), we identify their specific binding to distinct surface regions of the cellulose nanocrystals used. Surface regions featuring bulk defects (also referred to as “crystal-internal” defect sites) like cracks or voids were frequently used for binding (Figure 2A, indicated by arrows). However, most of the cellulosomes (~80%) were located at the small crystal ends (“tips”), as shown in Figure 2B. Preferred localization to the crystal tips might be explained by substrate

binding recognition of the predominant catalytic subunits of the cellulosome. The cellulosome from cellulose-grown culture of *C. thermocellum* comprises the cellobiohydrolase Cel48S as a major catalytic subunit.^{17,31} Cel48S is a main factor of the cellulosome's overall hydrolytic efficiency on crystalline cellulose,⁴² and its activity is directed toward the reducing chain ends.¹⁷ Just like crystal-internal defect sites, crystal tips are expected to expose a large amount of chain ends that can serve as sites for enzyme binding and attack.

The cellulosomes were occasionally located at the top surface of cellulose nanocrystals (Figure 2C; right panel). Typically, these cellulosomes were elongated in shape, thus covering most of the cellulose surface area available for their binding (Figure 2C; right panel). Binding solely at a nanocrystal's side wall for a noticeable period of time (≥ 1 min) was not observed. Clear distinction is thus drawn between the cellulosome and noncomplexed cellulases as regards their binding recognition of crystalline cellulose surfaces. In noncomplexed cellulases, crystalline cellulose degradation is primarily due to the activity of chain-end cleaving cellobiohydrolases.²⁸ We have shown in recent work that, on cellulose nanocrystals exactly comparable to the ones used here, the prototypical cellobiohydrolase Cel7A from *Trichoderma reesei* (*TrCel7A*) binds preferably to the crystals' side-wall surfaces. *TrCel7A* slides along these surfaces in one direction while performing its processive depolymerization activity on cellulose chains.²⁹

Tracking the Shapes of Individual Cellulosomes on the Cellulose Surface. Contrary to the rather compact shapes of the cellulosomes adsorbed on the surface of the wafers used for AFM observations (Figure S2A and S3), the cellulosomes bound on cellulose assumed strongly elongated, often filamentous shapes (Figure 2A,C). A switch in cellulosome shape, from compact to filamentous (Figure 2A and 2C), was demonstrated in time-lapse measurements, tracking individual cellulosomes bound on graphite in their approach on a nearby cellulose nanocrystal (Movie S1). The exact shape of the cellulose-bound cellulosomes was determined by the topology of the cellulose surface occupied by them. Cellulosomes bound at the small ends of cellulose nanocrystals adopted bent, sickle-like forms (Figure 2B, left panel), thus optimizing the exploitable contact area on the substrate end. Cellulosomes bound elsewhere in the nanocrystals assumed a variety of forms, as shown exemplarily in Figure 2A–C, apparently in an effort to maximize their contact with the locally accessible substrate material. Figure 2D shows distribution analysis for the different cellulosome shapes detected in the single-molecule experiments on cellulose nanocrystals. The results confirm the presence of elongated cellulosomes ($\text{DoD} \geq 3$), which are noticeably absent on the plain surface of the wafer (see Figure S3).

Once attached to cellulose, the cellulosomes remained bound locally for a timespan of several minutes (Movie S2). Interestingly, cellulosome binding at the top surface of the nanocrystals involved distinctly shorter cycles of adsorption/desorption (time range: ≤ 7.5 min) than binding at crystal tips or defect sites. There, the cellulosomes were bound typically for 10–20 min or even longer. Movie S1 (time range 0–5 min) shows a cellulosome located on a nanocrystal's top surface. Movie S2 shows a cellulosome bound to a crystal tip. Dynamic features of cellulosome binding to cellulose are thus distinguished clearly from those of the cellobiohydrolase *TrCel7A*. Determined under identical conditions as used

here except for a temperature of 25 °C, the average residence time of mobile *TrCel7A* enzymes on the nanocrystals' side walls is just 30 s or smaller.²⁹ The inherent multivalency of cellulose binding by the cellulosome, resulting from multiple protein modules interacting with the substrate surface simultaneously (Figures 2 and 3), is expected to promote an

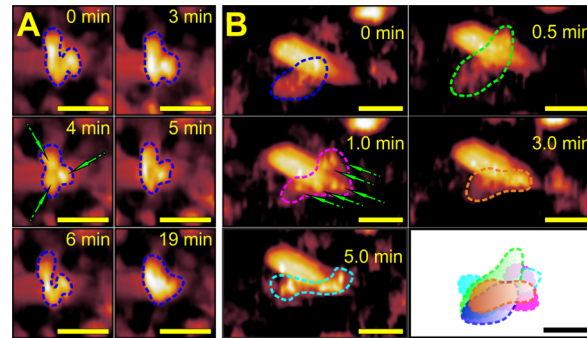


Figure 3. Visualization with ultrastructural resolution of the conformational flexibility of individual cellulosomes degrading cellulose nanocrystals. (A) Time-lapse AFM observation of a single cellulosome (outlined in blue) with varying shape and reorganized ultrastructure (indicated by arrows) adsorbed to a cellulose nanocrystal. Image acquisition rate was 0.5 min⁻¹, and images were taken from Movie S2. (B) Time-lapse AFM observation of a single cellulosome (outlined with colors) with partly resolved ultrastructure (indicated by arrows) adsorbing to a cellulose nanocrystal and subsequently varying its shape. Internal features are indicated by arrows. An overlay of the conformations assumed over the depicted time course is shown in the lower right panel. Image acquisition rate was 2.0 min⁻¹, and images were taken from Movie S1. All AFM experiments were conducted at 50 °C with a resolution of either 3 (A) or 2 (B) nm/pix, respectively. Scale bars are 50 nm.

enhanced residence time on the cellulose nanocrystals. Our direct measurements at single-molecule resolution thus support previous ideas^{43,44} of a lower dissociation rate of the cellulose-bound cellulosome as compared with cellulose-bound cellulases of the noncomplexed type. We note that anchorage in the bacterial cell wall is likely to pose additional restrictions on the dynamic interaction of the cellulosome with the cellulose surface. However, we suggest that the fundamental characteristics of substrate binding revealed here are relevant for cell-associated and nonassociated cellulose systems⁴⁵ alike.

Conformational Adaptability of the Cellulosome on the Cellulose Surface. Evidence that noncomplexed cellulases stay substantially shorter on the cellulose surface than cellulosomal complexes do suggest fundamental differences in strategy employed by the two enzyme systems to maintain biochemical synergy between their respective catalytic functionalities during the degradative process. Proximity ensures continued synergistic catalysis by the enzymes within cellulosomal complexes. To achieve the same effect, single enzymes have to rely on enhanced dynamics of their turnover on the cellulose surface. However, despite being immobile as a whole, the individual cellulosomes monitored over time exhibit a large degree of flexibility/adaptability in their ultrastructure, as exemplarily shown in Figure 3 and more completely visualized in Movie S1. The temporal resolution (~2 frames/min) of our time-lapse analysis was well suited to monitor such major, slow conformational/ultrastructural rearrangements during the prolonged residence time (≥ 10

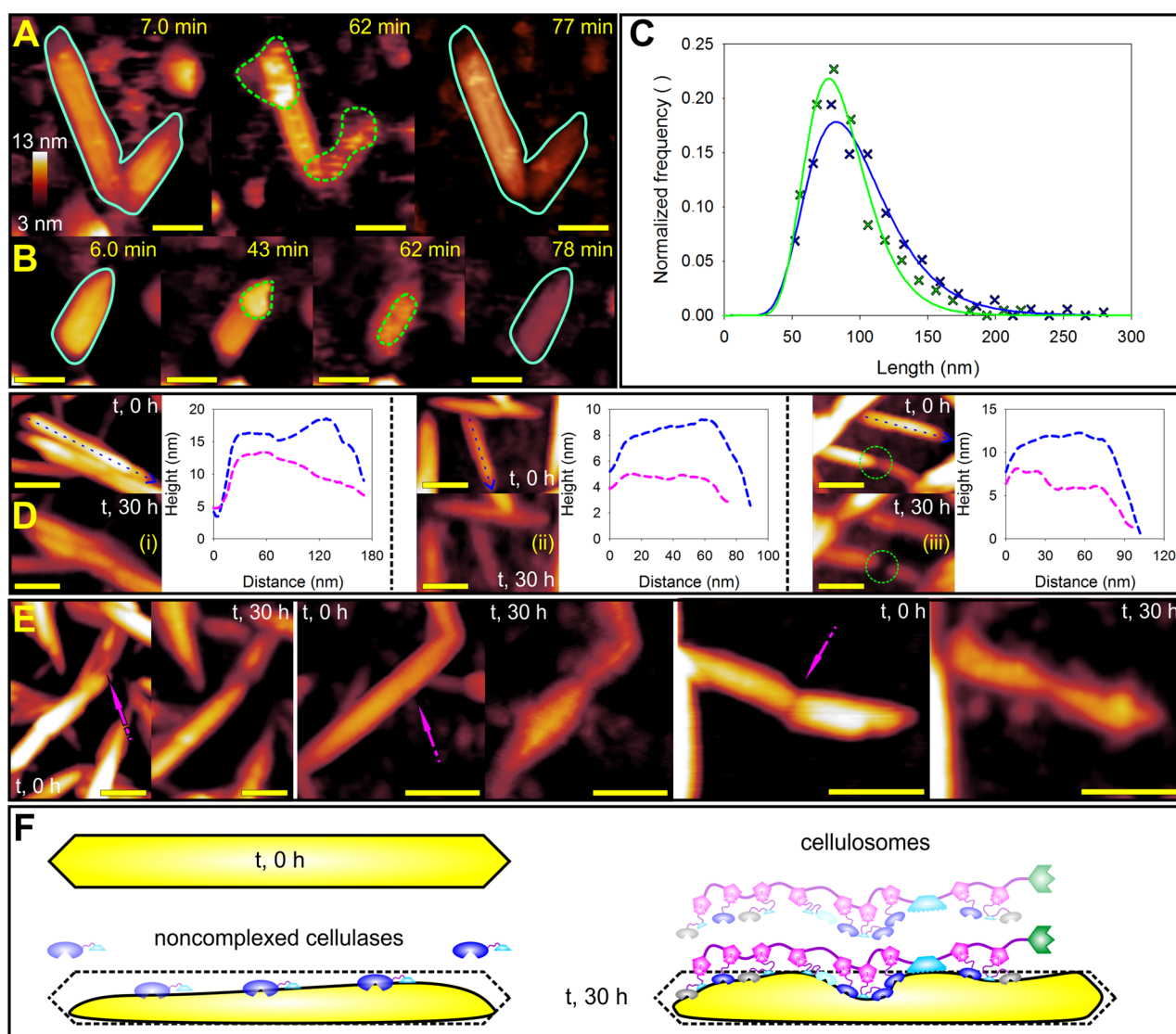


Figure 4. Mode of action of the cellulosome in deconstructing cellulose nanocrystals. (A, B) Snapshots from time-lapse AFM observation over 80 min of the cellulosomes degrading different cellulose nanocrystals at 50 °C. Exemplary cellulosomes associated with the cellulose nanocrystals are highlighted in green. The initial crystal perimeters are outlined in cyan projected onto the last image of the corresponding image sequence. Image acquisition rate was 0.5 min⁻¹, and a further degradation sequence employing a similar color pattern is provided in Movie S3. (C) Length distribution of ~250 cellulose nanocrystals before (blue) and after (green) 30 h of incubation with the cellulosomes. (D) Typical longitudinal degradation profiles of cellulose nanocrystals after 30 h of degradation by the cellulosome at 50 °C. Profiles were collected along the arrows before (blue) and after cellulosome activity (pink). (E) Visualization of typical attack patterns observed after cellulosome activity on internal sides on cellulose nanocrystals. (F) Schematic of the mechanisms by which a processive cellulase (cellobiohydrolase) of the noncomplexed type such as *TrCel7A* (left) ablates and cellulosomes (right) deconstruct a cellulose nanocrystal, respectively. On highly crystalline cellulose such as the cellulose nanocrystals used here, the activity of noncomplexed cellulases is largely dominated by the activity of the processive cellobiohydrolase. For simplicity, therefore, the noncomplexed cellulases are represented schematically by this single enzyme. A completely uniform false color scale (shown in panel A) was used throughout each image sequence (panel A, 3 to 13 nm; panel B, 3 to 16 nm; panel D, (i) 5 to 18 nm, (ii) 1 to 14 nm and (iii) 1 to 15 nm; panel E from left to right, 3 to 15 nm, 5 to 15 nm and 2 to 10 nm). Scale bars are 50 nm.

min) of individual cellulosomes on essentially the same position on the cellulose surface. The notion is further supported by evidence that some cellulosomes remain at the adsorbed position for minutes without major rearrangement of their ultrastructure (compare the more flexible cellulosomes from Movie S1 with the more rigid cellulosome in Movie S2). We wish to be clear in that monitoring of the fast internal dynamics¹⁵ of the cellulosome (ultra)structure was not a goal of the current study. In terms of spatial resolution, we were able to identify individual subunits as spherical particles with a diameter of about 10–20 nm (Figure S1). Based on tip-

deconvolution calculations and assuming similar heights for the individual subunits, our experimental setup (~5 nm AFM tip) was fully apt in principle to distinguish between different subunits. Collectively, therefore, these results suggest that, through fine-tuning of their mode of cellulose binding via temporal rearrangement of ultrastructure (Figure 3A), the cellulosomes might be able to effectively perpetuate catalytic synergy, via optimal juxtaposition of their enzymatic subunits and continuous repositioning as a whole (Figure 3B). Thus, deconstruction of the substrate surface could proceed efficiently.

Deconstruction of Cellulose Nanocrystals by the Cellulosome. Besides tracking the individual cellulosomes on cellulose, we were also able to capture the characteristic details of their activity in solid substrate deconstruction. Using time-lapse AFM image acquisition (Figure 4A,B; Movie S3), we reveal cellulosomes attacking cellulose nanocrystals at their ends. The crystals' originally plain ends become characteristically beveled in the degradative process (Figure 4A, Movie S3). Continued removal of material results in shortening of the crystals. Small nanocrystals of length ($\leq \sim 70$ nm) approximately that of the elongated cellulosome are thus degraded almost completely in the timespan analyzed (~ 70 –120 min; Figure 4A, smaller crystal; Figure 4B). Although the removal of cellulosic material is clearly visible, the removed volume of cellulosic material cannot be assessed quantitatively. This precludes determination of a specific activity of the enzyme directly from the AFM data.

Examining the same population of nanocrystals on prestructured wafers in a quantitative length-distribution analysis before and after 30 h of incubation in the presence of the cellulosomes, we show that the cellulosomes degrade the nanocrystals characteristically through the formation of shorter fragments. A fraction of the nanocrystals is eventually removed, which is shown by a $\sim 15\%$ decrease in the overall nanocrystal count after incubation. Note: we restricted our length analysis to nanocrystals of an aspect ratio of 5:1 or higher. Thus, we ensured that only single nanocrystals were analyzed and bias due to nanocrystal aggregates was avoided. As shown in Figure 4C, the analyzed population of cellulose nanocrystals features a right-skewed log-normal distribution with a mean crystal length of about 82 nm. After incubation, the mean crystal length is reduced to about 76 nm, and interestingly, we observed an increased abundance of intermediate-sized cellulose nanocrystals (~ 70 –80 nm). Notably, the postdegradation distribution is thinner, and the initial right-skew is significantly reduced because of a particular decrease in abundance of the large (≥ 200 nm) cellulose nanocrystals. Deconstruction of the cellulose nanocrystals both from the ends and through fissions within would explain the observed change in nanocrystal length distribution. Detailed analysis of the degradation of selected single nanocrystals, as exemplarily shown Figure 4D,E, provides clear direct evidence in support of this 2-fold mode of attack of the cellulosome.

As depicted in Figure 4D, besides degradation to form beveled ends in larger crystals (≥ 150 nm) as depicted in (i) and degradation across the whole crystal length in smaller crystals (ii), we also observe the cellulosome to cut nanocrystals internally, so that two shorter fragments are produced eventually (iii). The internal fissions are typically found at defect sites in the crystal surface, as seen in Figure 4D (iii), that were noted above to serve as prominent binding sites for the cellulosome. Removal of surface material accessible to the locally bound cellulosome results in the formation of a constricted segment with shallow hole in the crystal surface, as shown in Figure 4E (indicated by arrows). Continued attack in this region leads to localized thinning of the crystal width. This progresses until the crystal is eventually cut through. The distinct length-shortening mode of nanocrystals degradation revealed in Figure 4C thus arises from cellulosome attacks both at the crystals' ends and in their middle.

Experiments with noncomplexed cellulases (from the fungus *Trichoderma reesei*) serve to emphasize the unique mode of action of the cellulosomes in cellulose nanocrystal degradation.

The cellulases degrade the nanocrystals by ablating surface material equally in the whole lateral dimension (Figure S4A,B). Analyzing a population of about 200 single nanocrystals (Figure S4C), we observe a right-skewed log-normal distribution with a mean crystal length of about 83 nm. Activity of the cellulases results in a decrease in the mean length to about 77 nm. However, contrary to observations made with the cellulosomes (Figure 4C), the distribution from cellulase activity becomes broader and does not accumulate intermediate-sized nanocrystals (Figure S4C). Instead, the distribution broadening involves a relative increase in short (≤ 70 nm) and long (≥ 200 nm) nanocrystals. Therefore, noncomplexed cellulases are not particularly efficient in shortening cellulose nanocrystals, and their mode of nanocrystal deconstruction differs fundamentally from that of the cellulosome. Careful evaluation of cellulose nanocrystals incubated in the absence of cellulolytic enzymes showed no structural changes.

Generally, the cellulases lack the distinct, vertically directed activity of cellulose surface deconstruction that we show in this study to be a highly characteristic feature of the cellulosome. Thus, unlike the cellulosome (Figure 4C), the cellulases are not effective in degrading the cellulose nanocrystals by internal cleavages or cleavages from the ends (Figure S4). The proposed distinct modes of action of the two cellulolytic systems on cellulose nanocrystals are depicted schematically in Figure 4F. Note: although noncomplexed cellulases involve multiple cellulose-degrading activities working in synergy, their highly typical, ablative mode of removal of surface material in crystalline cellulose (Figure 4F) is governed by the action of the main cellobiohydrolase, which in *T. reesei* cellulases is Cel7A. We show that *Tr*Cel7A is also the dominant activity for the degradation of cellulose nanocrystals by the cellulases. Isolated *Tr*Cel7A is similarly efficient as the complete cellulase mixture in releasing soluble sugars from the cellulose nanocrystals (Figure S5A).

AFM data-based comparison of the cellulosome and the cellulases as regards their relative efficiency of cellulose nanocrystal degradation reveals that the cellulosome is particularly active on the smallest cellulose nanocrystals present (length $\leq \sim 70$ nm). Contrarily, such small nanocrystals are hardly attacked by the cellulases. Both enzyme systems show similar overall activity on the nanocrystals used, resulting in removal of $\sim 30\%$ of original cellulosic material in the crystals remaining in the analyzed surface area of the wafer. Using cellulose nanocrystals in liquid suspension, we find that both enzyme systems are active toward releasing soluble sugars (Figure S5B), with the cellulases being about 3-fold more efficient, in terms of conversion and specific activity, than the cellulosome at equivalent protein loading. However, cellulose nanocrystals show a pronounced tendency to form aggregates in suspension.⁴⁶ The decrease in enzyme-accessible cellulose surface area due to nanocrystal aggregation is expected to increase dependent on the enzyme size. Thus, potential bias against the relatively large cellulosome is introduced when the enzyme activity is evaluated from reaction in suspension. Therefore, this emphasizes the importance of studying the deconstruction activity of the cellulosome on single cellulose crystals.

CONCLUSIONS

A long elusive paradigm of deconstruction of crystalline cellulose by cellulosome nanomachines now unfolds. We show that dynamic adaptation of quaternary protein structure to

different substrate nanoscale morphologies, present originally in the cellulose and evolving locally during its degradation, is fundamental to the cellulosome's mechanism of action. By combining complementary cellulase modules on a flexible scaffold protein, the cellulosomes avoid the difficult task of orchestrating the exchange of noncomplexed cellulase modules on the cellulose surface. In conditions of enzyme limiting the cellulose degradation, as is likely the case when naturally predigested or suitably pretreated cellulosic materials are the substrates, complexed enzymes therefore offer a distinct advantage. Our analysis of single *C. thermocellum* cellulosomes degrading individual cellulose nanocrystals reveals intrinsic characteristics of the deconstruction process. A reductionist approach regarding the morphology of the cellulose substrate used (single cellulose nanocrystals compared to larger cellulose particles) is essential for the mechanistic study. However, it must necessarily exclude the influence of more complex substrate morphologies that are additionally very important in the bioconversion of technologically relevant (ligno)cellulose materials. The surface ablation mechanism utilized by noncomplexed cellulases contrasts with the distinct, microfibril cutting and shortening mechanism utilized by the cellulosomes (Figure 4F). Synergy between these basic degradation mechanisms might be exploited in the design of hybrid cellulase systems that combine free and complexed enzymes in a highly effective hydrolysis cocktail for cellulose bioconversion and for upcoming lignocellulose biorefinery applications.

METHODS

Detailed description of the materials and methods involved in the preparation and analysis of cellulose nanocrystals, AFM sample preparation, cellulosome production/purification, and enzymatic hydrolysis are provided in the [Supporting Information](#). Full details of the procedures of AFM measurement and of the AFM data analysis are provided. Results of time-lapse AFM studies are shown in [Movies S1–S3](#), and additional results are provided in [Figures S1–S8](#).

ASSOCIATED CONTENT

Supporting Information

The Supporting Information is available free of charge at <https://pubs.acs.org/doi/10.1021/acscentsci.0c00050>.

Movie S1: time lapse measurement, tracking individual cellulosomes bound on a cellulose nanocrystal ([AVI](#))

Movie S2: shows a cellulosome bound to a crystal tip ([AVI](#))

Movie S3: cellulosomes attacking and partially degrading a cellulose nanocrystal ([AVI](#))

Detailed description of the materials and methods involved in the preparation and analysis of cellulose nanocrystals, AFM sample preparation, cellulosome production/purification, and enzymatic hydrolysis ([PDF](#))

AUTHOR INFORMATION

Corresponding Authors

Bernd Nidetzky – Institute of Biotechnology and Biochemical Engineering, Graz University of Technology, 8010 Graz, Austria; Austrian Centre of Industrial Biotechnology, 8010 Graz, Austria; orcid.org/0000-0002-5030-2643; Email: bernd.nidetzky@tugraz.at

Harald Plank – Institute for Electron Microscopy and Nanoanalysis, Graz University of Technology, 8010 Graz, Austria; Graz Centre of Electron Microscopy, A-8010 Graz, Austria; orcid.org/0000-0003-1112-0908; Email: harald.plank@felmi-zfe.at

Authors

Manuel Eibinger – Institute of Biotechnology and Biochemical Engineering, Graz University of Technology, 8010 Graz, Austria

Thomas Ganner – Institute for Electron Microscopy and Nanoanalysis, Graz University of Technology, 8010 Graz, Austria

Complete contact information is available at:

<https://pubs.acs.org/10.1021/acscentsci.0c00050>

Author Contributions

¶(M.E., T.G.) These authors contributed equally to this work.

Notes

The authors declare no competing financial interest.

ACKNOWLEDGMENTS

This work was supported by the Austrian Science Funds (FWF Project P-24156-B21 to B.N.).

REFERENCES

- (1) Good, M. C.; Zalatan, J. G.; Lim, W. A. Scaffold proteins: hubs for controlling the flow of cellular information. *Science* **2011**, *332*, 680–686.
- (2) Langeberg, L. K.; Scott, J. D. Signalling scaffolds and local organization of cellular behaviour. *Nat. Rev. Mol. Cell Biol.* **2015**, *16*, 232–244.
- (3) Zhang, Y.; Hess, H. Toward rational design of high-efficiency enzyme cascades. *ACS Catal.* **2017**, *7*, 6018–6027.
- (4) Wheeldon, I.; Minteer, S. D.; Banta, S.; Barton, S. C.; Atanassov, P.; Sigman, M. Substrate channelling as an approach to cascade reactions. *Nat. Chem.* **2016**, *8*, 299–309.
- (5) Ellis, G. A.; Klein, W. P.; Lasarte-Aragonés, G.; Thakur, M.; Walper, S. A.; Medintz, I. L. Artificial multienzyme scaffolds: pursuing in vitro substrate channeling with an overview of current progress. *ACS Catal.* **2019**, *9*, 10812–10869.
- (6) Liu, Z.; Cao, S.; Liu, M.; Kang, W.; Xia, J. Self-Assembled Multienzyme Nanostructures on Synthetic Protein Scaffolds. *ACS Nano* **2019**, *13*, 11343–11352.
- (7) Artzi, L.; Bayer, E. A.; Moraïs, S. Cellulosomes: bacterial nanomachines for dismantling plant polysaccharides. *Nat. Rev. Microbiol.* **2017**, *15*, 83–95.
- (8) Fontes, C. M. G. A.; Gilbert, H. J. Cellulosomes: highly efficient nanomachines designed to deconstruct plant cell wall complex carbohydrates. *Annu. Rev. Biochem.* **2010**, *79*, 655–681.
- (9) Smith, S. P.; Bayer, E. A. Insights into cellulosome assembly and dynamics: from dissection to reconstruction of the supramolecular enzyme complex. *Curr. Opin. Struct. Biol.* **2013**, *23*, 686–694.
- (10) Xu, Q.; et al. Dramatic performance of *Clostridium thermocellum* explained by its wide range of cellulase modalities. *Sci. Adv.* **2016**, *2*, e1501254.
- (11) Moraïs, S.; Morag, E.; Barak, Y.; Goldman, D.; Hadar, Y.; Lamed, R.; Shoham, Y.; Wilson, D. B.; Bayer, E. A. Deconstruction of lignocellulose into soluble sugars by native and designer cellulosomes. *mBio* **2012**, *3*, e00508-12.
- (12) Molinier, A.-L.; Nouailler, M.; Valette, O.; Tardif, C.; Receveur-Bréchot, V.; Fierobe, H.-P. Synergy, structure and conformational flexibility of hybrid cellulosomes displaying various inter-cohesins linkers. *J. Mol. Biol.* **2011**, *405*, 143–157.
- (13) Czjzek, M.; Fierobe, H.-P.; Receveur-Bréchot, V. Small-Angle X-ray Scattering and Crystallography. *Methods Enzymol.* **2012**, *510*, 183–210.

- (14) Currie, M. A.; Cameron, K.; Dias, F. M. V.; Spencer, H. L.; Bayer, E. A.; Fontes, C. M. G. A.; Smith, S. P.; Jia, Z. Small angle X-ray scattering analysis of *Clostridium thermocellum* cellulose N-terminal complexes reveals a highly dynamic structure. *J. Biol. Chem.* **2013**, *288*, 7978–7985.
- (15) Barth, A.; Hendrix, J.; Fried, D.; Barak, Y.; Bayer, E. A.; Lamb, D. C. Dynamic interactions of type I cohesin modules fine-tune the structure of the cellulose of *Clostridium thermocellum*. *Proc. Natl. Acad. Sci. U. S. A.* **2018**, *115*, E11274–E11283.
- (16) Bomble, Y. J.; Beckham, G. T.; Matthews, J. F.; Nimlos, M. R.; Himmel, M. E.; Crowley, M. F. Modeling the self-assembly of the cellulose enzyme complex. *J. Biol. Chem.* **2011**, *286*, 5614–5623.
- (17) Resch, M. G.; Donohoe, B. S.; Baker, J. O.; Decker, S. R.; Bayer, E. A.; Beckham, G. T.; Himmel, M. E. Fungal cellulases and complexed cellulosomal enzymes exhibit synergistic mechanisms in cellulose deconstruction. *Energy Environ. Sci.* **2013**, *6*, 1858.
- (18) Resch, M. G.; et al. Clean fractionation pretreatment reduces enzyme loadings for biomass saccharification and reveals the mechanism of free and cellulosomal enzyme synergy. *ACS Sustainable Chem. Eng.* **2014**, *2*, 1377–1387.
- (19) Bayer, E. A.; Lamed, R.; Himmel, M. E. The potential of cellulases and cellulosomes for cellulosic waste management. *Curr. Opin. Biotechnol.* **2007**, *18*, 237–245.
- (20) Gunnoo, M.; et al. Nanoscale engineering of designer cellulosomes. *Adv. Mater.* **2016**, *28*, 5619–5647.
- (21) Gilbert, H. J. Celluloses: Microbial nanomachines that display plasticity in quaternary structure. *Mol. Microbiol.* **2007**, *63*, 1568–1576.
- (22) Nash, M. A.; Smith, S. P.; Fontes, C. M.; Bayer, E. A. Single versus dual-binding conformations in cellulosomal cohesin–dockeerin complexes. *Curr. Opin. Struct. Biol.* **2016**, *40*, 89–96.
- (23) Bernardi, R. C.; Durner, E.; Schoeler, C.; Malinowska, K. H.; Carvalho, B. G.; Bayer, E. A.; Luthey-Schulten, Z.; Gaub, H. E.; Nash, M. A. Mechanisms of nanonewton mechanostability in a protein complex revealed by molecular dynamics simulations and single-molecule force spectroscopy. *J. Am. Chem. Soc.* **2019**, *141*, 14752–14763.
- (24) Hammel, M.; Fierobe, H.-P.; Czjzek, M.; Kurkal, V.; Smith, J. C.; Bayer, E. A.; Finet, S.; Receveur-Brechet, V. Structural basis of cellulose efficiency explored by small angle X-ray scattering. *J. Biol. Chem.* **2005**, *280*, 38562–38568.
- (25) Boisset, C.; Chanzy, H.; Henrissat, B.; Lamed, R.; Shoham, Y.; Bayer, E. A. Digestion of crystalline cellulose substrates by the *Clostridium thermocellum* cellulose: structural and morphological aspects. *Biochem. J.* **1999**, *340*, 829–835.
- (26) Bayer, E. A.; Shimon, L. J. W.; Shoham, Y.; Lamed, R. Celluloses—structure and ultrastructure. *J. Struct. Biol.* **1998**, *124*, 221–234.
- (27) Igarashi, K.; Uchihashi, T.; Koivula, A.; Wada, M.; Kimura, S.; Okamoto, T.; Penttila, M.; Ando, T.; Samejima, M. Traffic jams reduce hydrolytic efficiency of cellulase on cellulose surface. *Science* **2011**, *333*, 1279–1282.
- (28) Payne, C. M.; Knott, B. C.; Mayes, H. B.; Hansson, H.; Himmel, M. E.; Sandgren, M.; Ståhlberg, J.; Beckham, G. T. Fungal cellulases. *Chem. Rev.* **2015**, *115*, 1308–1448.
- (29) Eibinger, M.; Sattelkow, J.; Ganner, T.; Plank, H.; Nidetzky, B. Single-molecule study of oxidative enzymatic deconstruction of cellulose. *Nat. Commun.* **2017**, *8*, 894.
- (30) Lamed, R.; Bayer, E. Celluloses from *Clostridium thermocellum*. *Methods Enzymol.* **1988**, *160*, 472–482.
- (31) Gold, N. D.; Martin, V. J. J. Global view of the *Clostridium thermocellum* cellulose revealed by quantitative proteomic analysis. *J. Bacteriol.* **2007**, *189*, 6787–6795.
- (32) Ding, S.-Y.; Liu, Y.-S.; Zeng, Y.; Himmel, M. E.; Baker, J. O.; Bayer, E. A. How does plant cell wall nanoscale architecture correlate with enzymatic digestibility? *Science* **2012**, *338*, 1055–1060.
- (33) Fierobe, H.-P.; Bayer, E. A.; Tardif, C.; Czjzek, M.; Mechaly, A.; Bélaïch, A.; Lamed, R.; Shoham, Y.; Bélaïch, J.-P. Degradation of cellulose substrates by cellulose chimeras. *J. Biol. Chem.* **2002**, *277*, 49621–49630.
- (34) Mayer, F.; Coughlan, M. P.; Mori, Y.; Ljungdahl, L. G. Macromolecular organization of the cellulolytic enzyme complex of *Clostridium thermocellum* as revealed by electron microscopy. *Appl. Environ. Microbiol.* **1987**, *53*, 2785–2792.
- (35) Doi, R. H.; Kosugi, A. Celluloses: plant-cell-wall-degrading enzyme complexes. *Nat. Rev. Microbiol.* **2004**, *2*, 541–551.
- (36) García, R. *Amplitude Modulation Atomic Force Microscopy*; Wiley-VCH Verlag GmbH & Co. KGaA: Weinheim, Germany, 2010.
- (37) Hansma, H. G.; Hoh, J. H. Biomolecular imaging with the atomic force microscope. *Annu. Rev. Biophys. Biomol. Struct.* **1994**, *23*, 115–140.
- (38) Dufrêne, Y. F.; Ando, T.; Garcia, R.; Alsteens, D.; Martinez-Martin, D.; Engel, A.; Gerber, C.; Müller, D. J. Imaging modes of atomic force microscopy for application in molecular and cell biology. *Nat. Nanotechnol.* **2017**, *12*, 295–307.
- (39) Brunecky, R.; et al. Revealing nature's cellulase diversity: the digestion mechanism of *Caldicellulosiruptor bescii* CelA. *Science* **2013**, *342*, 1513–1516.
- (40) Brunecky, R.; Subramanian, V.; Yarbrough, J. M.; Donohoe, B. S.; Vinzant, T. B.; Vanderwall, T. A.; Knott, B. C.; Chaudhari, Y. B.; Bomble, Y. J.; Himmel, M. E.; Decker, S. R.; et al. Synthetic fungal multifunctional cellulases for enhanced biomass conversion. *Green Chem.* **2020**, *22*, 478.
- (41) Jiang, F.; Kittle, J. D.; Tan, X.; Esker, A. R.; Roman, M. Effects of sulfate groups on the adsorption and activity of cellulases on cellulose substrates. *Langmuir* **2013**, *29*, 3280–3291.
- (42) Olson, D. G.; et al. Deletion of the Cel48S cellulase from *Clostridium thermocellum*. *Proc. Natl. Acad. Sci. U. S. A.* **2010**, *107*, 17727–17732.
- (43) Boraston, A. B.; McLean, B. W.; Chen, G.; Li, A.; Warren, R. A. J.; Kilburn, D. G. Co-operative binding of triplicate carbohydrate-binding modules from a thermophilic xylanase. *Mol. Microbiol.* **2002**, *43*, 187–194.
- (44) Boraston, A. B.; Bolam, D. N.; Gilbert, H. J.; Davies, G. J. Carbohydrate-binding modules: fine-tuning polysaccharide recognition. *Biochem. J.* **2004**, *382*, 769–781.
- (45) Artzi, L.; Dadosh, T.; Milrot, E.; Moraïs, S.; Levin-Zaidman, S.; Morag, E.; Bayer, E. A. Colocalization and disposition of celluloses in *Clostridium clariflavum* as revealed by correlative superresolution imaging. *mBio* **2018**, *9*, e00012-18.
- (46) Eibinger, M.; Ganner, T.; Bubner, P.; Rošker, S.; Kracher, D.; Haltrich, D.; Ludwig, R.; Plank, H.; Nidetzky, B. Cellulose surface degradation by a lytic polysaccharide monooxygenase and its effect on cellulase hydrolytic efficiency. *J. Biol. Chem.* **2014**, *289*, 35929–35938.